Journal of Solid State Chemistry **147,** 527–535 (1999)
Article ID jssc.1999.8412, available online at http://www.idealibrary.com on IDEAL®

A Novel Family of Layered Bismuth Compounds

I. The Crystal Structures of $Pb_{0.6}Bi_{1.4}Cs_{0.6}O_2Cl_2$ and $Pb_{0.6}Bi_{3.4}Cs_{0.6}O_4Cl_4$

D. O. Charkin,* P. S. Berdonosov,* A. M. Moisejev,* R. R. Shagiakhmetov,* V. A. Dolgikh,* and P. Lightfoot†,[1]

*Department of Chemistry, Moscow State University, Moscow 119899 GSP-3 Russia; and †School of Chemistry, University of St. Andrews, St. Andrews, KY16 9ST Fife, United Kingdom

Received February 5, 1999; in revised form May 14, 1999; accepted May 27, 1999

Twenty new multinary bismuth oxide halogenides have been prepared and characterized by means of X-ray powder diffraction. In their structures, fluorite-related layers are separated by CsCl-related metal–halogen sheets. Four compounds are isostructural to $Ca_3Bi_5CsO_8Cl_6$ which has an intergrowth structure between a Sillén *X*1 phase and a novel structural element ("*Y*2"). Another four compounds crystallize in a novel structure type which is an intergrowth between the *X*2 Sillén phase and the *Y*2 element. The remaining 12 compounds adopt the *Y*2 structure which is also a new structure type. In the former two families, Bi^{3+} can be substituted only by Pb^{2+}; in the latter family, Bi^{3+} can also be substituted by Na^+ and Ba^{2+} . The crystal structure of $Pb_{0.6}Bi_{3.4}Cs_{0.6}O_4Cl_4$ (intergrowth *X*2*Y*2 structure) has been solved from single crystal data, and the structure of $Pb_{0.6}Bi_{1.4}Cs_{0.6}O_2Cl_2$ (*Y*2 structure) has been solved from powder data. Crystal chemical relationships to Sillén phases are discussed.

INTRODUCTION

Multinary bismuth, lanthanoid, and actinoid oxides, oxide halogenides, chalcogenides, pnictides, etc. with layered structures constitute a large class of compounds which demonstrate unusual and interesting properties, such as high-temperature superconductivity, ferroelectricity, ionic conductivity, and catalytic activity. Their crystal chemistry is also very rich with unusual structures, there being an array of individual families. However, a detailed classification based on structural peculiarities has been hitherto worked out only for the so-called Sillén phases (1). Their general classification can be suggested for the whole array on the basis of structure types, from which the structures of layers constituting the whole structure are derived. In many of the compounds in the discussion, positively charged (cationic) layers possess a fluorite-related structure. These layers are interleaved with negatively charged (anionic) layers derived from different structure types. Table 1 gives a brief classification of the structures containing fluorite-like layers (a) and shows how this classification can be expanded to other layered families, where fluorite-like layers are not involved (b).

At the moment, the family of compounds with fluorite-type cationic layers seems to be the most numerous, at least concerning the number of structure types of anionic counterlayers. Moreover, it also looks incomplete. To predict a new combination of layers derived from two structure types (one per "cationic" and one per "anionic" layer), three "compatibility criteria" are sound: (i) charge balance, (ii) redox (chemical) compatibility, and (iii) geometrical compatibility. An excellent example of how these criteria should be applied to structure modeling of new complicated intergrowth structures is given in (18), where the correctness of the approach was confirmed by subsequent synthesis of a vast new family of mixed-layered bismuth oxyhalides.

The *a* (and *b*) parameters of the fluorite-related layers usually fall within the range 3.8–4.2 Å ($\approx a_{\text{fluorite}}/\sqrt{2}$); therefore, the parameters of the anionic layer should be of the same value (or *n* or $n\sqrt{2}$ times larger). Of the simplest cubic or tetragonal structures with $a \approx 4$ Å which can serve as initial ones for building anion blocks, CsCl seems to be a very reliable candidate since it has already been involved in some related layered families (see Table 1, b). Therefore, a set of layered structures with alternating layers derived from the CaF_2 and CsCl structures is likely to exist.

Quite recently, such a possibility was proved by synthesis of a novel calcium–bismuth–cesium oxide chloride, $Ca_3Bi_5CsO_8Cl_6$ (19). In its structure, the fluorite-related $[(Ca, Bi)_2O_2]$ layers are separated by single chlorine ion layers, as well as by $[Cs_{0.5}Cl_2]$ metal–halogen layers with the structure derived from that of CsCl. Thus, the whole structure can be considered as an intergrowth between a Sillén *X*1 phase (as a tetragonal version of $CaBiO_2Cl$) and a novel $Ca_{0.5}Bi_{1.5}Cs_{0.5}O_2Cl_2$ "building block" which can

[1]To whom correspondence should be addressed. E-mail: pl@st-and.ac.uk.

0022-4596/99 $30.00

TABLE 1
Classification of Multinary Compounds with Layered Structures

Structure type of the cationic layer	Structure type of the anionic layer	Representatives	Ref.
	a. Structures containing fluorite-related layers		
CaF_2	—	α-PbO, α-SnO	(1)
CaF_2	single anion sheets	Sillén phases $X1$ and $X2$	(1)
CaF_2	molecular anions	$Bi_2O_2CO_3$, $Pb_2F_2SO_4$	(1, 2)
CaF_2	anionic chains	Bi_2SiO_5, Bi_2GeO_5	(3)
CaF_2	$CaTiO_3$	Aurivillius phases	(4)
CaF_2	NaCl	Sillén phases $X3$ and $X4$	(1, 5)
CaF_2	*anti*-CaF_2	LaOAgS, ZrSiCuAs	(6, 7)
CaF_2	ZnS (sphalerite)	$(LaO)_2CdSe_2$	(8)
CaF_2	$LaNiO_2$	Nd_2CuO_4, $(Y, Ce)_3SrCuFeO_9$	(9, 10)
CaF_2	ReO_3	$Pb_2Nb_3O_5F_7$	(11)
	b. Examples of other structures		
anti-NbO	*anti*-CaF_2	$UCuP_2$	(12)
NaCl	*anti*-CaF_2	$GdCRu_2B_2$, $(LaN)_3Ni_2B_2$	(13, 14)
NaCl	$CaTiO_3$	HTSC cuprates	(15)
CsCl	$CaTiO_3$	$Pb_4Fe_3O_8Cl$	(16)
NbO	NaCl	$K_nNb_4(O, F)_{n+5}$	(17)

be classified as a "fluorite–CsCl" layer sequence (Fig. 1). Two questions arise: (i) whether such a "building element" can exist by itself but not in an intergrowth compound only, and (ii) if other intergrowth structures involving this element can be found.

By analogy with Sillén phases $X1$, $X2$, etc, where the numeral index denotes number of anionic layers separating fluorite-related layers (1), the structure of the novel "building block" may be denoted as $Y2$, where the numeral index denotes the number of halogen sublayers in the $[Q_{1-x}Z_2]$ CsCl-related block.

In the present paper, we describe synthesis and crystal structure modeling and determination for 20 novel multinary bismuth oxide halogenides which belong to the supposed family.

STRUCTURE MODELLING

The Y2 Structure

Supposing complete occupancies for all atomic sites, the chemical formula of a compound with $Y2$ structure should be written as $[(Me, Bi)_2O_2][QZ_2]$, where Me is a substituent for Bi (further (Me, Bi) will be denoted as M), Q is a large cation in the cubic void of the CsCl-related layer, and Z stands for halogen.[2] Taking into account nonstoichiometry of the anionic block in $Ca_3Bi_5CsO_8Cl_6$, one can suppose the stoichiometry to be $[M_2O_2][Q_{1-x}Z_2]$. In the latter case, the charge of the fluorite-related layer should be noninteger, which can be achieved due to the unique ability of Bi^{3+} ions in the $[(Me, Bi)_2O_2]$ fluorite-related layers to be substituted by aliovalent ions in different ratios. In Sillén phases, several substituents are known; according to their chemical nature, they can be divided into four groups: (i) Pb^{2+}, (ii) Cd^{2+}, (iii) Li^+ and Na^+, and (iv) Ca^{2+}, Sr^{2+}, and Ba^{2+}. One can suppose these ions to be substituents for Bi^{3+} in the designed family as well; oxychlorides being usually isostructural to oxybromides and oxyiodides, all halogens (actually excluding fluorine) should be tried and, finally, Cs^+ can perhaps be replaced by Rb^+ or K^+.

The cell parameters for a $Y2$ structure (let $Me = Ca$, $Q = Cs$, and $Z = Cl$) can be easily calculated (Fig. 1): $a \approx \sqrt{2}/2 \cdot a(Ca_3Bi_5CsO_8Cl_6) = 3.9$ Å (not considering superstructure), $c \approx c(Ca_3Bi_5CsO_8Cl_6) - c(CaBiO_2Cl) = 20.4$ Å (the c parameter for $CaBiO_2Cl$ is taken from an early work (20), where its diffraction pattern was indexed as tetragonal). The highest-symmetry space group is $I4/mmm$.

Intergrowth Structures

Among layered oxyhalides (mainly Sillén phases), the most common element of intergrowth structures is that of $X2$ (PbFCl, or BiOCl type). The chemical formula for $X2Y2$ compounds should be $[M_2O_2][Z]_2[M_2O_2][Q_{1-x}Z_2] \equiv M_4O_4Q_{1-x}Z_4$; for $X2X2Y2$ it should be $M_6O_6Q_{1-x}Z_6$. For $X1Y2$ structures, the formula is $[M_2O_2][Z][M_2O_2][Q_{1-x}Z_2] \equiv M_4O_4Q_{1-x}Z_3$. The compound $Ca_3Bi_5CsO_8Cl_6$ ($\equiv Ca_{1.5}Bi_{2.5}Cs_{0.5}O_4Cl_3$, $x = 0.5$) belongs to this family. One could also expect existence of $X3Y2$ compounds with the layer sequence $[M_2O_2][M'_{1-x}Z_3][M_2O_2][Q_{1-y}Z_2]$ (M' filling the octahedral voids in triple halogen layers), etc.

[2] We use the symbol Z for halogens instead of the conventional X to distinguish between the halogen symbol and the X symbol used for notation of the Sillén phases and the Y symbol introduced here.

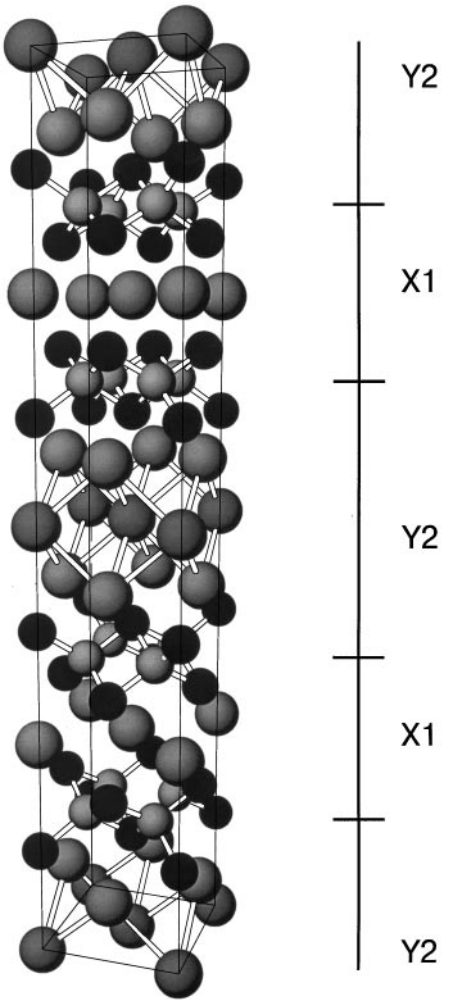

FIG. 1. The crystal structure of $Ca_3Bi_5CsO_8Cl_6$: $X1$ and $Y2$ blocks are shown.

EXPERIMENTAL

A Search for Y2 Compounds

In the current work, one representative was tried for each group of substituents for Bi^{3+} (see above): Pb^{2+}, Cd^{2+}, Na^{+}, and Ba^{2+}.

In the first step of the search, to estimate actual stoichiometry and to look for possible homogeneity areas, Pb^{2+} was tried as a substituent for Bi^{3+}. Stoichiometric mixtures of high-purity (> 99.99%) PbO, BiOCl, and CsCl (dehydrated at 150°C for 2 hr) according to composition $Pb_xBi_{2-x}Cs_xO_2Cl_2$ with $x = 0.5, 0.6, 0.7, 0.8, 1.0$ were well ground, placed in silica ampoules, sealed under vacuum, and heated at 610 ± 10°C for 10 days. No special precautions were taken when weighing and grinding the precursors. The annealed samples looked almost colorless (with a yellow or bluish grey tint) and were well crystallized, except that with $x = 1$, which was dark yellow powder. The X-ray diffraction data (Guinier camera FR-552, Enraf-Nonius, $CuK\alpha_1$, germanium used as internal standard) showed all of the samples except the latter to contain a group of lines attributed to a new phase with a detectable homogeneity area, since a shift of the lines compared to the $x = 0.6$ sample was found in those with $x = 0.5$ and $x = 0.7$. The X-ray diffraction pattern (XDP) of $Pb_{0.6}Cs_{0.6}Bi_{1.4}O_2Cl_2$ was completely indexed by the TREOR90 (21) program in tetragonal symmetry with $a = 3.9101(5)$ Å and $c = 20.975(4)$ Å (Table 2). No superstructure observed for the X_1Y_2 phase $Ca_3Bi_5CsO_8Cl_6$ ($a = \sqrt{2} \cdot a_0$) could be found. Systematic extinctions pointed to a body-centered cell, the highest symmetry group being $I4/mmm$ (the only extinction rule found was $h + k + l = 2n$). The M_{20} value for $I4/mmm$ space group is 58.

The cell parameters of the new compound fitted well with those proposed when modeling the structure (somewhat larger since Pb^{2+} is more voluminous than Ca^{2+}). Further experiments have shown the homogeneity area of the new compound to lie between $x \approx 0.55$ and $x \approx 0.65$.

A compound with the proposed cell parameters being obtained, other possible combinations of elements were tested with a stoichiometry $Me^{II}_{0.6}Bi_{1.4}Q_{0.6}O_2Z_2$ or $M^{I}_{0.3}Bi_{1.7}Q_{0.6}O_2Z_2$ (Me^{I} = Na, Me^{II} = Pb, Cd, Ba, Q = K,

TABLE 2
Indexed X-Ray Diffraction Pattern for $Pb_{0.6}Bi_{1.4}Cs_{0.6}O_2Cl_2$

2θ	d (Å)	Intensity	hkl	10^4 (d^2_{obs})	10^4 (d^2_{calc})
8.449	10.5	m	002	91.4	91.4
23.161	3.836	st	011	679	676
25.543	3.484	w	006	824	822
26.110	3.410	vst	013	860	859
31.282	2.856	st	015	1225	1225
32.318	2.768	vst	110	1305	1307
33.482	2.674	m	112	1398	1398
41.632	2.168	w	116	2129	2130
43.239	2.091	vw	00$\underline{10}$	2288	2286
46.360	1.9569	st	020	2612	2614
47.207	1.9237	m	022	2702	2705
47.802	1.9011	w	118	2767	2769
52.401	1.7446	w	00$\underline{12}$, 121	3286	3291, 3290
53.617	1.7079	w	026	3428	3436
54.990	1.6684	vw	11$\underline{10}$	3592	3592
57.009	1.6140	st	125	3839	3838
58.932	1.5659	vw	028	4078	4076
61.327	1.5103	vw	127	4384	4387
65.275	1.4282	w	02$\underline{10}$	4903	4900
67.697	1.3829	w	220	5229	5227
68.329	1.3716	w	222	5316	5319
73.512	1.3872	vw	12$\underline{11}$	6036	6032
73.888	1.2816	w	033	6089	6086
76.436	1.2450	w	035	6451	6452
77.021	1.2370	m	130	6535	6534
77.672	1.2283	vw	132	6628	6625

TABLE 3
Unit Cell Parameters of the New Multinary Bismuth Oxyhalides

Compound	a (Å)	c (Å)	Z	Type of superstructure
		Structure type $Y2$		
$Pb_{0.6}Bi_{1.4}Cs_{0.6}O_2Cl_2$	3.912(1)	20.92(1)	2	none
$Pb_{0.6}Bi_{1.4}Cs_{0.6}O_2Br_2$	3.962(1)	21.61(1)	2	
$Pb_{0.6}Bi_{1.4}Rb_{0.6}O_2Cl_2$	3.899(1)	20.06(1)	2	
$Pb_{0.6}Bi_{1.4}Rb_{0.6}O_2Br_2$	3.957(1)	20.98(1)	2	
$Na_{0.3}Bi_{1.7}Cs_{0.6}O_2Cl_2$	3.953(1)	20.79(1)	2	
$Na_{0.3}Bi_{1.7}Cs_{0.6}O_2Br_2$	3.927(1)	21.54(1)	2	
$Na_{0.3}Bi_{1.7}Rb_{0.6}O_2Cl_2$	3.943(1)	19.77(2)	2	
$Na_{0.3}Bi_{1.7}Rb_{0.6}O_2Br_2$	3.916(2)	20.85(1)	2	
$Ba_{0.6}Bi_{1.4}Cs_{0.6}O_2Cl_2$	3.970(1)	20.74(2)	2	
$Ba_{0.6}Bi_{1.4}Cs_{0.6}O_2Br_2$	4.041(2)	21.60(2)	2	
$Ba_{0.6}Bi_{1.4}Rb_{0.6}O_2Cl_2$	3.966(1)	19.81(1)	2	
$Ba_{0.6}Bi_{1.4}Rb_{0.6}O_2Br_2$	4.025(1)	20.91(1)	2	
		Structure type $X1Y2$		
$Pb_{1.5}Bi_{2.5}Cs_{0.5}O_4Cl_3$	5.557(2)	32.83(2)	4	$a = \sqrt{2^*}a_0$
$Pb_{1.5}Bi_{2.5}Cs_{0.5}O_4Br_3$	5.628(2)	34.26(4)	4	$c = 2^*c_0$
$Pb_{1.5}Bi_{2.5}Rb_{0.5}O_4Cl_3$	5.559(3)	32.39(2)	4	
$Pb_{1.5}Bi_{2.5}Rb_{0.5}O_4Br_3$	5.612(2)	33.69(2)	4	
		Structure type $X2Y2$		
$Pb_{0.6}Bi_{3.4}Cs_{0.6}O_4Cl_4$	3.897(1)	35.44(2)	2	none
$Pb_{0.6}Bi_{3.4}Cs_{0.6}O_4Br_4$	3.945(2)	37.38(2)	2	
$Pb_{0.6}Bi_{3.4}Rb_{0.6}O_4Cl_4$	3.897(1)	34.85(4)	2	
$Pb_{0.6}Bi_{3.4}Rb_{0.6}O_4Br_4$	3.938(1)	36.99(1)	2	

Rb, Cs, Z = Cl, Br, J). The starting compounds were PbO, CdO, Bi_2O_3, BiOZ, and alkali metal halogenides (preliminarily dehydrated). In the case of barium compounds, the $BaBiO_2Z$ precursors were prepared first.[3] The synthetic conditions were the same as described above or (in the case of Na and Ba compounds) the annealing temperature was 700 ± 20°C. X-ray data indicated formation of several isostructural phases; their cell parameters are given in Table 3. In the case of iodides or cadmium samples, the $Y2$ compounds were not formed. In the $Pb_{0.6}Bi_{1.4}K_{0.6}O_2Cl_2$ sample, traces of some colored admixture were present. The XDP looked similar to that of $Pb_{0.6}Bi_{1.4}Cs_{0.6}O_2Cl_2$, and most of the lines could be indexed by analogy with cell parameters $a = 3.931(1)$ Å, $c = 21.74(1)$ Å. However, these cell parameters are significantly larger than those expected for a K^+-$Y2$ compound (see Table 3), taking into account that $r_{K^+} < r_{Rb^+}$. Therefore, it looks likely that this compound has a structure different from, though related to, that of $Pb_{0.6}Bi_{1.4}Cs_{0.6}O_2Cl_2$.

[3] $BaBiO_2Cl$ was prepared as described in (22). $BaBiO_2Br$ was prepared under the same conditions, but the reaction mixture was annealed in dynamic vacuum (0.1 Torr), to avoid oxidation. The compound proved to be isostructural to $BaBiO_2Cl$ with cell parameters $a = 5.9690(1)$ Å, $b = 13.3180(2)$ Å, and $c = 5.7492(1)$ Å.

A Search for New Intergrowth Compounds on the Basis of the Y2 Structure

Among multinary Bi–Me oxide halogenides, the intergrowth compounds are known only for Me = Ca, Sr, Pb, and Cd (1); therefore, in this work, novel intergrowth oxide halogenides were sought among lead compounds.

The X1Y2 compounds. Supposing lead-containing $X1Y2$ compounds to have approximately the same stoichiometry as their calcium analog, we obtained, under the same synthetic conditions, single-phase $Pb_{1.5}Bi_{2.5}Q_{0.5}O_4Z_3$ compounds for Q = Rb and Cs, and Z = Cl and Br. Their X-ray patterns were indexed by analogy with the calculated pattern of $Ca_3Bi_5CsO_8Cl_6$. All $X1Y2$ compounds crystallize in tegragonal symmetry with the same type of superstructure as found for $Ca_3Bi_5CsO_8Cl_6$ ($a = \sqrt{2} \cdot a_0$, $c = 2 \cdot c_0$; see Table 3). These compounds also have homogeneity areas, but they are more narrow than those for the $Y2$ compounds; for instance, the sample of composition $Pb_{1.57}Bi_{2.43}Cs_{0.57}O_4Br_3$ contained an $X1Y2$ phase together with a significant amount of some cubic phase with a rather small cell parameter (3.4378(8) Å). The unit cell of the latter is primitive, and the simplest suggestion is that it has a CsCl-type structure with statistical distribution of cations (Pb^{2+}, Bi^{3+}, and Cs^+), anions ($O^{2-} + Br^-$), and perhaps vacancies, over the corresponding sites.

The X2Y2 compounds. During the search, a series of samples was annealed with a composition $Pb_{0.6}Bi_{3.4}Q_{0.6}O_4Z_4$ (Q = Rb, Cs; Z = Cl, Br) which is expected for the $X2Y2$ intergrowths. The XDP of $Pb_{0.6}Bi_{3.4}Rb_{0.6}O_4Cl_4$ contained reflections with $d \approx 17.5$ Å and $d \approx 8.5$ Å, which fitted well with the expected c value of ≈ 34.8 Å. A strong reflection with $d \approx 2.78$ Å was chosen as (110), and that with $d \approx 17.5$ Å as (002). The XDP was completely indexed with the a and c parameters calculated from the chosen interplanar spacings (see Table 4). As in the case of $Pb_{0.6}Bi_{1.4}Cs_{0.6}O_2Cl_2$, no superstructure was found. The XDPs of all the other compounds were indexed by analogy with that of $Pb_{0.6}Bi_{1.4}Rb_{0.6}O_4Cl_4$, with cell parameters given in Table 3.

All attempts to prepare intergrowth compounds with $X3Y2$ or $X2X2Y2$ structure (corresponding to $Pb_{1.85}Bi_{2.9}Cs_{0.6}O_4Cl_5$ or $Pb_{0.6}Bi_{5.4}Cs_{0.6}O_6Cl_6$ compositions) have been unsuccessful.

STRUCTURE DETERMINATION

The Y2 Structure

A single-phase sample of composition $Pb_{0.6}Bi_{1.4}Cs_{0.6}O_2Cl_2$ was prepared as described above. A lot of transparent yellowish platelets were found in the sample. However, their Laue photographs contained only diffuse lines instead of sharp spots. Therefore, we attempted to solve the structure

TABLE 4
Indexed X-Ray Diffraction Pattern for $Pb_{0.6}Bi_{3.4}Rb_{0.6}O_4Cl_4$

2θ	d (Å)	Intensity	hkl	10^4 (d^2_{obs})	10^4 (d^2_{calc})
5.005	17.6	w	002	32.1	32.9
10.107	8.74	w	004	131	131
22.953	3.871	m	011	667	667
24.095	3.690	m	013	734	733
26.195	3.399	vst	015	866	864
32.463	2.756	vst	110	1317	1317
32.892	2.721	vw	112	1351	1350
34.102	2.627	m	114	1449	1449
41.747	2.162	vw	11$\underline{10}$	2140	2140
46.578	1.9482	st	020	2635	2633
46.898	1.9357	w	022	2669	2666
47.796	1.9014	m	024	2766	2765
49.292	1.8471	w	026, 11$\underline{14}$	2931	2930, 2931
52.507	1.7413	w	121	3298	3300
53.035	1.7252	w	123	3360	3366
54.220	1.6903	st	125	3500	3498
57.961	1.5898	m	129	3957	3959
60.278	1.5341	vw	02$\underline{14}$	4249	4248
67.938	1.3786	m	220	5262	5267
68.970	1.3604	w	224	5403	5399
74.234	1.2764	vw	035	6138	6131
77.384	1.2321	w	039, 130	6587	6592, 6584
78.245	1.2207	vw	134	6711	6715

TABLE 5
Experimental Conditions and Crystallographic Data for $Pb_{0.6}Bi_{1.4}Cs_{0.6}O_2Cl_2$

	Experiment 1 [(002) and (004) included]	Experiment 2 [(002) and (004) excluded]
Formula weight	1199.07	1199.07
Color	grayish white	grayish white
Crystal system	tetragonal	tetragonal
Space group	$I4/mmm$ (no. 139)	$I4/mmm$ (no. 139)
Cell parameters		
a (Å)	3.9140(1)	3.9101(1)
c (Å)	20.8629(5)	20.8633(4)
V (Å^3)	319.0(3)	310.0(2)
Z	2	2
Calculated density	6.820(5)	6.820(4)
Diffractometer	STOE STADI/P	STOE STADI/P
Radiation and wavelength	Cu$K\alpha_1$ ($\lambda = 1.54056$ Å)	Cu$K\alpha_1$ ($\lambda = 1.54056$ Å)
2Θ range (degrees)	5–100	20–100
Mode of refinement	full profile	full profile
Texture axis and parameter	[001]0.581(6)	[001] 0.82(1)
Number of reflexions	72	70
Number of free variables	9	13
R_p	0.135	0.063
R_{wp}	0.130	0.081
R_I	0.083	0.047
R_F		0.030

from powder data which were collected on a STOE STADI/P diffractometer (starch was added to the sample to suppress preferred orientation). The experimental conditions are given in Table 5. All calculations were made using the CSD package software (23).

Based on the systematic extinctions, several space groups were possible, of which the lowest symmetrical ones were chosen initially. All attempts to refine the proposed model in $I4$, $I4mm$, $I\bar{4}m2$, or $I4/m$ diverged or gave intolerable interatomic distances. Meanwhile, refinement in $I\bar{4}$ converged to satisfactory results. Taking preferred orientation (using the March–Dollase model) into account yielded $R_I = 0.083$, $R_p = 0.135$, and $R_{wp} = 0.130$; however, lower values of R factors could not be reached. All attempts to split cesium positions, by analogy with $Ca_3Bi_5CsO_8Cl_6$, in different space groups resulted in insignificant success or led to divergence. When analyzing atomic parameters we found additional symmetry elements which finally led to highest symmetry group $I4/mmm$. The refinement in this space group resulted in slightly better reliability factors but slightly larger thermal parameters.

Examination of the difference profile led us to a conclusion that the main source of errors to be the strong (002) peak which belongs to the (00l) series most influenced by preferred orientation. It was also found that a weak (004) reflection (which belongs to the same series) overlaps with the amorphous halo of the starch. Therefore, we attempted to refine the model after having excluded the (002) and (004) peaks from the data set, using the RIETAN program (24). The solution in $I4/mmm$ rapidly converged to $R_I = 0.047$, $R_F = 0.030$ without significant change of positional parameters. The details of both experiments are summarized in Tables 5 (crystallographic data) and 6 (positional and thermal parameters). Selected bond distances and angles are given in Table 7. Rietveld refinement plots are given in Figs. 2a and 2b, respectively. A view of the crystal structure is given in Fig. 3a.

TABLE 6
Final Atomic Parameters for $Pb_{0.6}Bi_{1.4}Cs_{0.6}O_2Cl_2$

		Experiment 1		Experiment 2	
Atom	Site	xyz	B	xyz	B
$Pb_{0.3}Bi_{0.7}$	4e	0 0 0.1903(1)	0.53(3)	0 0 0.1903(5)	2.6(9)
$Cs_{0.6}$	2a	0 0 0	3.1(2)	0 0 0	5.5(1)
Cl	4e	$\frac{1}{2}\frac{1}{2}$ 0.1100(4)	2.8(3)	$\frac{1}{2}\frac{1}{2}$ 0.1128(2)	2.8(2)
O	4d	$\frac{1}{2}0\frac{1}{4}$	5.6(8)	$\frac{1}{2}0\frac{1}{4}$	1.6[a]

[a]Not refined in the experiment.

TABLE 7
Selected Bond Distances and Angles for $Pb_{0.6}Bi_{1.4}Cs_{0.6}O_2Cl_2$

	Distance		Distance		Angle
M–O[a]	2.318(1)	×4	M–O–M	×2	114.98(4)
M–Cl	3.230(5)	×4		×4	106.79(4)
Cs–Cl	3.590(6)	×8			

[a] $M = Pb_{0.3}Bi_{0.7}$.

The X2Y2 Structure

During the search for $X2X2Y2$ compounds, the $Pb_xBi_{1-x}Cs_xOCl$ samples with $x = 0.05$–0.10 decomposed when occasionally overheated with liberation of metallic bismuth. However, these samples were the only ones in which well-shaped single crystals were found. One of these appeared to be tetragonal with $a \approx 3.90$ Å, $c \approx 35$ Å, which are the expected cell parameters for an $X2Y2$ compound.

The crystal structure was solved using the TEXSAN program (25) in space group $I4/mmm$. The details of the single-crystal experiment are listed in Table 8. Supposing the structure to be an intergrowth of $Pb_{0.6}Bi_{1.4}Cs_{0.6}O_2Cl_2$ and BiOCl structures, approximate atomic positions were estimated and taken as a structure model. The solution converged rapidly to the R value of 0.11; however, all attempts to improve the reliability factors failed, as in the case of $Pb_{0.6}Bi_{1.4}Cs_{0.6}O_2Cl_2$. The atomic parameters are listed in Table 9. Selected bond distances are given in Table 10. The crystal structure of the compound is represented in Fig. 3b.

STRUCTURE DESCRIPTION

The Y2 Structure

The crystal structure of $Pb_{0.6}Bi_{1.4}Cs_{0.6}O_2Cl_2$ (see Fig. 3a) can be regarded as alternation of metal–oxygen and metal–halogen sheets perpendicular to [001]. The fluorite-related metal–oxygen ("cationic") sheet is constructed of edge-sharing OM_4 tetahedra, M = Pb, Bi. The tetrahedra are slightly flattened along the $\bar{4}$ axis, which is typical for fluorite-related layers in multinary bismuth oxide halogenides and oxide chalcogenides. The metal–halogen ("anionic") layer is built up of $CsCl_8$ cubes which are, on the contrary, considerably stretched along the 4 axis. The Cs–Cl distance of 3.59 Å is only slightly longer than that in CsCl (3.56 Å), despite nonstoichiometry. The coordination polyhedron of M can be regarded as an Archimedean antiprism, one base being formed by four oxygens and the other by four chlorine atoms. The M–O (2.32 Å) and M–Cl distances (3.23 Å) are comparable to those in $PbBiO_2Cl$ (2.27 and 3.47 Å) and BiOCl (2.32 and 3.05 Å, respectively; see (1) and references therein). The coordination polyhedron of the chlorine atom can be considered as a strongly distorted M_4Cs_4 cube.

The X2Y2 Structure

The structure of $Pb_{0.6}Bi_{3.4}Cs_{0.6}O_4Cl_4$ (Fig. 3b) is an intergrowth of BiOCl and $Pb_{0.6}Bi_{1.4}Cs_{0.6}O_2Cl_2$ structures. It is layered as well, but the layer sequence is more complicated: $-[M_2O_2]-[Cl]_2-[M_2O_2]-[Cs_{0.6}Cl_2]-[M_2O_2]-\cdots$. In this structure, the OM_4 tetrahedra are more significantly distorted, the M–O distances being nonequal. The coordination polyhedra of Cs, $M1$, and Cl1 are the same as in the previous structure; the polyhedra of $M2$ and Cl2 are similar to those in BiOCl (a capped antiprism and a tetragonal pyramid).

DISCUSSION

The results of our experiments demonstrate that we have found a new family of layered bismuth oxyhalides with a novel structure element as a building block. In all the compounds, fluorite-related $[M_2O_2]$ layers are separated by $[Q_{1-x}Z_2]$ metal–halogen layers with the structure derived from that of caesium chloride. The structural features of the former seem to be very similar to those in Sillén phases, concerning the geometry and chemical nature of the ions substituting for Bi^{3+}. Some differences, however, can be noticed. In addition to our inability to introduce Cd^{2+} into fluorite-related layers (which is by all means possible in Sillén phases), no cation ordering can be found, at least in the $Y2$ and $X2Y2$ structures. For the $X1$ Sillén phases with composition $Me^{II}BiO_2Z$, cation ordering seems now to be a rule rather than an exception (22, 26). For instance, while $BaBiO_2Cl$ demonstrates cation ordering in the $[BaBiO_2^+]$ layers (orthorhombic symmetry), no ordering can be found in the $[Ba_{0.6}Bi_{1.4}O_2^{+1.4}]$ layers in $Ba_{0.6}Bi_{1.4}Cs_{0.6}O_2Cl_2$ (tetragonal symmetry). When the Me-to-Bi ratio is smaller ($Me^{I}Bi_3O_4Z_2X1$ compounds), cation ordering is absent, but fewer Me^+ cations can be used as substituents: though the ionic radii of Ba^{2+} and K^+ do not differ as drastically as those of Ba^{2+} and Li^+ ($r_{Ba^{2+}} = 1.42$ Å, $r_{K^+} = 1.51$ Å, $r_{Li^+} = 0.92$ Å (27)), $BaBiO_2Cl$ and $LiBi_3O_4Cl_2$ exist while $KBi_3O_4Cl_2$ does not. However, in the $Y2$ phases, without cation ordering, Ba^{2+} and K^+ have equal opportunity to be introduced into the fluorite-related layers, and one can expect existence of $Y2$ compounds $K_{0.3}Bi_{1.7}Q_{0.6}O_2Z_2$.

For the tetragonal phase in $Pb_{0.6}Bi_{1.4}K_{0.6}O_2Cl_2$ sample, the XDP is similar to that of the Rb $Y2$ compound; however, both parameters are larger than those of the latter while, since Rb^+ is larger than K^+, they should be, of course, less. Tetragonal cell parameters of $a \approx 4$ Å and $c \approx 22$ Å are also typical for $X3$ Sillén phases, so we suppose the actual stoichiometry of the potassium compound to be $Pb_xBi_{2-x}O_2K_{1-y}Cl_{3-x-y}$, K^+ ions filling the octahedral

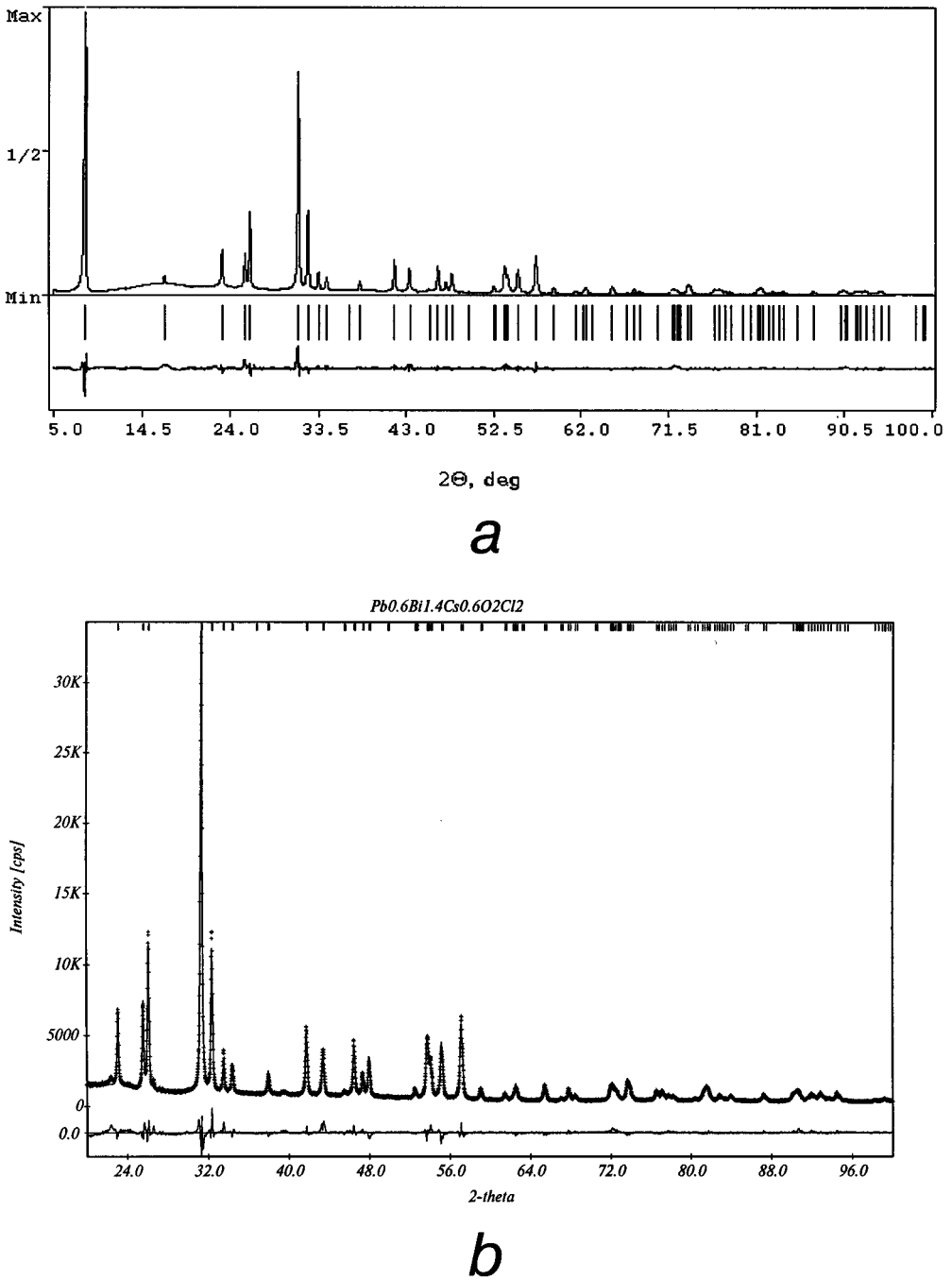

FIG. 2. Final Rietveld refinement plots for $Pb_{0.6}Bi_{1.4}Cs_{0.6}O_2Cl_2$ (a) with (002) and (004) included, (b) with (002) and (004) omitted.

voids in the triple anion layer while the lead ions substitute, as usual, the Bi^{3+} ions in the fluorite-related layers. The potassium ions are too large to enter octahedral voids in the stoichiometric triple chloride anion layer; therefore, it may be supposed that the "inner" chlorine sublayer is also filled incompletely, to make room for the K^+ ions. Investigations aimed at finding whether this supposition is correct are in progress now.

There is a peculiarity in the trends in the change of cell parameters of *Y*2 phases when proceeding from Cl to Br. For the lead-containing compounds, the *a* parameter increases for both Rb and Cs compounds. However, for sodium-substituted ones the *a* parameter decreases. A similar behavior (decrease of *a* cell parameters when passing to a larger anion) was found for lanthanide oxyhalides LnO*Z* where $a(\mathrm{LnOBr}) > a(\mathrm{LnOI})$ (1).

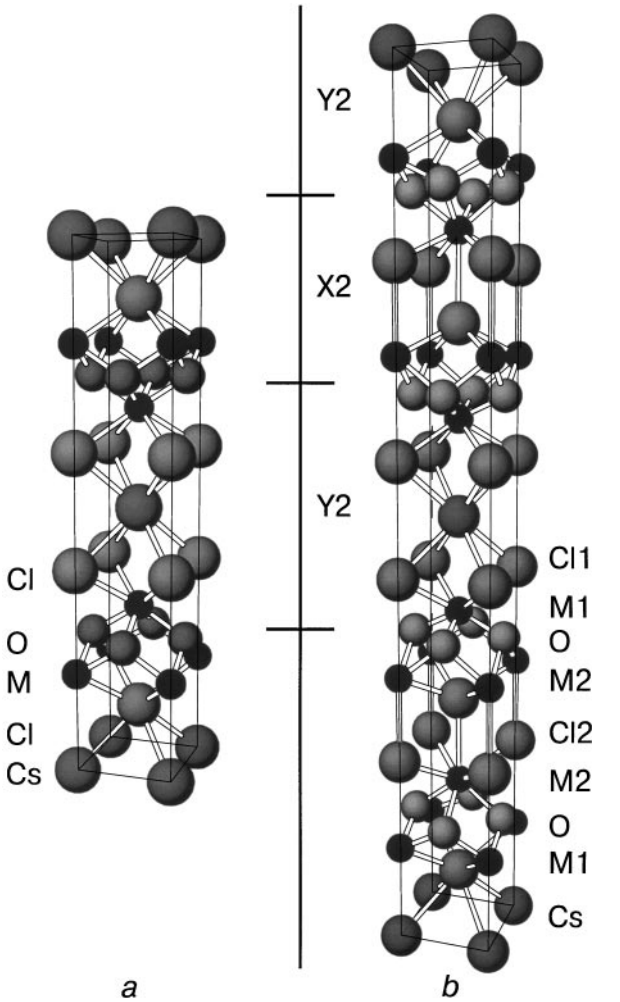

FIG. 3. The crystal structures of (a) the $Y2$ compound $Pb_{0.6}Bi_{1.4}Cs_{0.6}O_2Cl_2$ and (b) the $X2Y2$ compound $Pb_{0.6}Bi_{3.4}Cs_{0.6}O_4Cl_4$; the $X2$ and $Y2$ blocks are shown.

One can also mention that, all other ions being the same, the *a* cell parameters of Rb and Cs $Y2$ halides differ marginally (by ca. 0.01 Å). This means the parameters are almost independent of the nature of the Q^+ ion, as the completely ionic $[Q_{1-x}Z_2]$ layer is very flexible compared to the covalent-bonded $[M_2O_2]$ layer. In the $X1Y2$ and $X2Y2$ compounds with two $[M_2O_2]$ layers per one $[Q_{1-x}Z_2]$ layer, the difference in *a* parameters becomes negligible or disappears. It should be mentioned that the *a* parameters of the $X2Y2$ chlorides are very close to that of BiOCl (3.892 Å). The remaining difference of 0.005 Å can be explained by presence of larger Pb^{2+} ions in the $X2Y2$ compounds. The *c* cell parameters of the $X2Y2$ compounds coincide with the geometrical sum of *c* parameters of the $Y2$ and $X2$ compounds within ca. 0.2 Å, which is less than 1%.

Despite the very good agreement between observed and calculated *c* cell parameters of the $X2Y2$ compounds, there are sufficient indications of some disorder in the layer stacking, the first of them being rather high residuals in our single-crystal experiment (Table 8). A similar phenomenon was earlier found by Sillén upon refinements of structures like $X2X2X3$ (28). We suppose the following reason that disorder in layer stacking so easily occurs in complicated intergrowth structures of layered oxyhalides. Usually, in these structures the metal atoms in the $[M_2O_2]$ layers are distributed over two or more crystallographic sites. Of the latter, some are occupied by Bi^{3+} ions only ("pure Bi^{3+} positions"), while the others contain Bi^{3+} together with substituting Me^{n+} ions ("substituted positions"). (In more detail, this cation ordering is considered in (29)). Therefore, a difference in chemical nature occurs between different metal–oxygen layers, which is more or less pronounced, dependent on the *Me*-to-Bi ratio. We believe this difference to be the reason that ordering in layer sequence occurs at all, and the less pronounced this difference is, the more

TABLE 8
Experimental Conditions and Crystallographic Data for $Pb_{0.6}Bi_{3.4}Cs_{0.6}O_4Cl_4$

Formula weight	2240.80
Color	yellow
Crystal system	tetragonal
Space group	*I*4/*mmm* (no. 139)
Cell parameters	
a (Å)	3.897(1)
c (Å)	35.535(9)
V (Å^3)	540.0(4)
Z	2
Calculated density	6.893(6)
Diffractometer	Rigaku AFC7S
Radiation	$MoK\alpha_1$
Range in *h*, *k*, *l*	0–5, 0–3, 0–24
Transmission (ψ-scan) min, max	0.14; 1.00
Number of observed reflexions	232
Number of free parameters	18
R	0.112
R_w	0.079
S	9.2

TABLE 9
Final Atomic Parameters for $Pb_{0.6}Bi_{3.4}Cs_{0.6}O_4Cl_4$

Atom	Site	*xyz*	*B*
*M*1[a]	4*e*	0 0 0.1112(2)	1.61(7)
*M*2	4*e*	0 0 0.3183(2)	1.63(7)
$Cs_{0.6}$	2*a*	0 0 0	2.7(4)
Cl1	4*e*	$\frac{1}{2}\frac{1}{2}$0.066(1)	2.2(4)
Cl2	4*e*	0 0 0.217(1)	1.6(3)
O	8*g*	$\frac{1}{2}$0 0.139(2)	1.7(10)

[a]For explanations, see text.

TABLE 10
Selected Bond Distances for $Pb_{0.6}Bi_{3.4}Cs_{0.6}O_4Cl_4$

Bond	Distance		Bond	Distance	
*M*1–O	2.19(3)	×4	*M*2–Cl2	3.05(2)	×4
*M*1–Cl1	3.18(2)	×4	*M*2–Cl2	3.59(2)	×1
*M*2–O	2.46(4)	×4	Cs–Cl1	3.62(2)	×8

disorder arises in the layer stacking. In the Sillén phases, the *Me*-to-Bi ratio varies from 1 : 1 (e.g., in $PbBiO_2Cl$) to 1 : 11 (in $Ca_{1.25}Bi_{5.5}O_6Cl_7$; the Ca^{2+} ions in the octahedral voids not accounted for). In the case of $Pb_{0.6}Bi_{3.4}Cs_{0.6}O_4Cl_4$, the Pb-to-Bi ratio is 1 : 5.7, which is rather low and thus enables some disorder in the structure. In the Ca-*X*1*Y*2 compound, the ratio is relatively high (1 : 1.7), so stacking faults, if they exist, could not be observed. We consider stacking faults to be the main reason for high *R* factors in our single-crystal experiment.

The above-mentioned cation ordering over different crystallographical sites in our case (structure of $Pb_{0.6}Cs_{0.6}Bi_{3.4}O_4Cl_4$) is demonstrated by the sufficient difference in the *M*1–O and *M*2–O distances: it should be underlined that cation ordering in the $[(Pb, Bi)_2O_2]$ fluorite-related layers cannot be determined by conventional X-ray or neutron diffraction methods but only deduced from the *M*–O bond distances (29). Since Pb^{2+} is larger that Bi^{3+} one can conclude that the *M*1 position which is oriented toward $[Cs_{0.6}Cl_2]$ layers is a "pure Bi^{3+} position," while the *M*2 position oriented toward the double halogen layers contains both Pb^{2+} and Bi^{3+}. A situation in which a higher-charged metal sublayer is situated more closely to the less-charged anion layer may seem unusual; however, a similar behavior was found for $SrBi_2O_3Cl_2$ (*X*1*X*1*X*2) and $SrBi_3O_4Cl_3$ (*X*1*X*2) compounds (28), where it was shown that Sr^{2+} ions are situated in the metal sublayers oriented to double, not single, chlorine layers. The Cs–Cl distances change marginally when proceeding from *Y*2 to *X*2*Y*2 structure, as is expected for purely ionic bonds.

Nonetheless, the above-mentioned flexibility of $[Q_{1-x}Z_2]$ layers cannot explain the absence of the corresponding iodides. However, related metal–anion sheets in *X*3 and *X*4 Sillén phases are also well known for anion = Cl, Br, S, and Se, but not for I and Te (1, 30). It may also be that the expected *a* parameters for the *Y*2 iodides are beyond the tolerance limit for the fluorite-related layers. One can suppose that iodides may be obtained when Bi^{3+} ions are substituted by some very large cations such as K^+ or even Rb^+. These investigations are in progress now.

ACKNOWLEDGMENTS

Professor L. A. Aslanov is thanked for valuable discussions. This work was supported by the INTAS foundation (grant 97-1324) and the Russian Foundation for Basic Researches (grant 98-03-82559a).

REFERENCES

1. V. A. Dolgikh and L. N. Kholodkovskaya. *Russ. J. Inorg. Chem.* **37,** 488 (1992).
2. A. R. Kampf, *Amer. Miner.* **76,** 278 (1991).
3. J. Ketterer and V. Krämer, *Neues Jahrb. Miner. Monatsch.* 13 (1986).
4. B. Aurivillius, *Arkiv Kemi* **1,** 463, 499 (1949); B. Aurivillius, *Arkiv Kemi* **2,** 519 (1950) .
5. R. Céolin and N. Rodier, *Acta Crystallogr. B* **32,** 1476 (1976).
6. M. Palazzi and S. Jaulmes, *Acta Crystallogr. B* **37,** 1337 (1981).
7. V. Johnson and W. Jeitschko, *J. Solid State Chem.* **11,** 161 (1974).
8. I. Yu. Baranov, V. A. Dolgikh, and B. A. Popovkin, *Russ. J. Inorg. Chem.* **41,** 1819 (1996).
9. H. Müller-Buschbaum and W. Wollschläger, *Z. Anorg. Allg. Chem.* **414,** 76 (1975).
10. R. Li, K. Tang, Y. Qian, and Z. Chen, *Mater. Res. Bull.* **27,** 349 (1992).
11. J. Pannetier and P. Batail, *J. Solid State Chem.* **39,** 15 (1981).
12. H. Noël, Z. Zolnierek, D. Kaczorowski, and R. Troc, *J. Less-Common. Met.* **132,** 327 (1987).
13. J. Ye, T. Shishido, T. Kimura, T. Matsumoto, and T. Fukuda, *Acta Crystallogr. C* **52,** 2652 (1996).
14. R. J. Cava, H. W. Zandbergen, B. Batlogg, H. Eisaki, H. Takagi, J. J. Krajevski, W. F. Peck, Jr, E. M. Gyorgy, and S. Uchida, *Nature* **372,** 245 (1994).
15. M. A. Subramanian, J. C. Calabrese, and C. C. Torardi, *Nature* **332,** 420 (1988).
16. O. Savborg, *J. Solid State Chem.* **57,** 143 (1985).
17. A. V. Arakcheyeva, V. V. Grinevich, and G. U. Lubman, "Proceedings of the 1st National Crystal Chemical Conference, Chernogolovka, Russia, May 24–29," p. 7, 1998.
18. J. F. Ackerman, *J. Solid State Chem.* **62,** 92 (1986).
19. K. D. M. Harris, W. Ueda, and J. M. Thomas, *Angew. Chem Int. Ed.* **27,** 1364 (1988).
20. S. S. Lopatin, *Russ. J. Inorg. Chem. Russ. Ed.* **32,** 1694 (1987).
21. P.-E. Werner, L. Eriksson, and M. Westdahl, *J. Appl. Crystallogr.* **18,** 360 (1985).
22. M. A. Kennard, J. Darriet, J. Grannec, and A. Tressaud, *J. Solid State Chem.* **117,** 201 (1995).
23. L. G. Aksel'rud, Yu.N. Grin,' P. Yu. Zavalij, V. K. Pecharski, and V. S. Fundamentski, "Thes. Report on 12th European Crystallography Meeting, Moscow," p. 155, 1989.
24. F. Izumi, *J. Crystallogr. Soc. Jpn.* **27,** 23 (1985).
25. TEXSAN, Crystal Structure Analysis Package, Molecular Structure Corporation, 1992.
26. S. M. Fray, C. J. Milne, and P. Lightfoot. *J. Solid State Chem.* **128,** 115 (1997).
27. R. D. Shannon, *Acta Crystallogr. A* **32,** 761 (1976).
28. L. G. Sillén, Inaugural Dissertation, Stockholm, 1940.
29. P. S. Berdonosov, D. O. Charkin, V. A. Dolgikh, and B. A. Popovkin, *Russ. J. Inorg. Chem.* **44** (in press).
30. M. Guittard, S. Benazeth, J. Dugué, S. Jaulmes, M. Palazzi, P. Laruelle, and J. Flahaut, *J. Solid State Chem.* **51,** 227 (1984).